Development of Polarized e+ Beams for Future Linear Colliders

M. CHIBA, A. ENDO, R. HAMATSU, M. HIROSE, T. HIROSE,
M. IRAKO, N. KAWASAKI, T. KUMITA, Y. KURIHARA,
T. MATSUMOTO, H. NAKABUSHI, T. OKUGI, T. OMORI,
Y. TAKEUCHI, M. WASHIO, J. YANG and M. YOSHIOKA

National Laboratory for High Energy Physics, 1995

KEK Reports are available from:

Technical Information & Library
National Laboratory for High Energy Physics
1-1 Oho, Tsukuba-shi
Ibaraki-ken, 305
JAPAN

Phone:	0298-64-5136	
Telex:	3652-534	(Domestic)
	(0)3652-534	(International)
Fax:	0298-64-4604	
Cable:	KEK OHO	
E-mail:	Library@kekvax.kek.jp	(Internet Address)

Development of polarized e^+ beams for future linear colliders

M. Chiba[1], A. Endo[2], R. Hamatsu[1], M. Hirose[2], T. Hirose[1]
M. Irako[1], N. Kawasaki[1], T. Kumita[1], Y. Kurihara[3]
T. Matsumoto[1], H. Nakabushi[2], T. Okugi[1], T. Omori[3]
Y. Takeuchi[3], M. Washio[2], J. Yang[1], M. Yoshioka[3]

[1]Department of Physics, Tokyo Metropolitan University.
Hachioji, Tokyo 192-03, Japan
[2]Research and Development Center.
Sumitomo Heavy Industries, Ltd. (SHI)
63-30, Yuuhigaoka, Hiratsuka, Kanagawa 254, Japan
[3]National Laboratory for High Energy Physics (KEK)
Tsukuba, Ibaraki 305, Japan

Abstract
We have so far been carrying out systematic investigations to create polarized e^+ on the basis of two new methods. One method is to use β^+ decay of radioactive neuclei with short life-time produced with a proton cyclotron and the other method is to use e^+e^- pair creation from polarized γ beams made through backward Compton scattering of laser lights. Here we describe technical details on productions of polarized e^+ and measurements of the polarization. The experiments of producing polarized e^+ will soon start. Although the e^+ intensity is not sufficiently high, we will acquire lots of know-how for further development of polarized e^+ sources with high quality which will possibly be applied to future linear colliders.

1 Introduction

Since development of polarized e^- source has been successfully done [1] [2] [3] [4], we can expect a highly polarized e^- beam in future linear colliders, for which we require higher performance on the e^- source than for the SLC. When we discuss physics at future linear colliders in this literature, we always assume that e^- beam is highly polarized.

Questions that arise next are;
- Can we also polarize an e^+ beam?
- If an answer is YES, what can we gain from the collider in which both of e^- and e^+ beams are polarized?

From the point of view of high energy physics, the polarized e^+ beam should play important roles in next generation e^+e^- colliders. First, we discuss cases that we study physics of the Standard Model in which e^- and e^+ always interact in the helicity combination of $e_R^+ e_L^-$ (RL) and $e_L^+ e_R^-$ (LR), except in the case of two photon interaction. Therefore if we choose the helicity of e^- (note helicity equals chirality in massless limit), the helicity of e^+, which can interact with the e^-, is automatically selected. However, even in this case, the polarization of e^+ plays a particular role. If e^+ beam is not polarized, half of e^+ in the beam cannot interact because half of collisions occurs in the "wrong" combination, such as $e_R^+ e_R^-$ (RR) and $e_L^+ e_L^-$ (LL). Then polarization of e^+ beam gives us a factor two increase of an effective luminosity if both e^- and e^+ beams have 100% polarization, because we can always choose the "correct" combination of helicities (RL and LR). In actual colliders, whose beams are not 100% polarized, it is convenient to define the quantity C corresponding to the fraction of "correct" helicity combinations of e^- and e^+ in the beams: $C = \frac{1}{2}(1 - P_+ P_-)$ where P_+ and P_- are polarizations of e^+ and e^- beams, respectively ($P_\pm = 1$ means the polarization of 100% right handed helicity beam). We can also increase an effective polarization $P_{eff} = \frac{P_- - P_+}{1 - P_- P_+}$ as shown in the comparison of two cases, namely (i) 90% left-handed e^- beam and a non-polarized e^+ beam and (ii) 90% left-handed e^- beam and 80% polarization of a right-handed e^+ beam. The latter gains a factor 1.7 increase of an effective luminosity than the former; $\frac{C(P_-=-0.9, P_+=0.8)}{C(P_-=-0.9, P_+=0)} = 1.7$ and hence the latter has effective polarization of 99% while the former has 90%.

In addition, the polarization of both e^+ and e^- beams will suppress drastically the systematic error on measurement of the left-right asymmetry of a cross section;

$$A_{LR} = \frac{\sigma(LR) - \sigma(RL)}{\sigma(LR) + \sigma(RL)} .$$

When we measure A_{LR}, most part of systematic errors arises from the polarization measurement of a beam in the case of single beam polarization. If we polarize both of e^+ and e^- beams, propagation of errors from the polarization measurements to A_{LR} can be drastically supressed[5].

In studying new physics beyond the Standard Model, the polarization of an e^+ beam would play much essential roles, because some models allow interactions in "wrong" combinations (RR and LL). The supersymmetric extension of the Standard Model, for example, allows reactions such as, $e_R^+ e_R^- \to \tilde{e}_R^- \tilde{\chi}^+ \bar{\nu}_e$, and $e_L^+ e_L^- \to \tilde{e}_R^+ \tilde{\chi}^- \nu_e$, where $\tilde{e}^\pm$ and $\tilde{\chi}^\pm$ stand for a scaler electron and a chargino, respectively. Thus, by choosing the helicities of e^- and e^+ beams as RR or LL, we can study these interactions free of the backgrounds from the Standard Model interactions. $e.g.$ $e_R^+ e_L^- \to W^+ W^-$, $e_L^+ e_R^- \to W^+ W^-$. Furthermore, if the mass of $\tilde{e}^\mp$ are smaller than that of $\tilde{\chi}^\pm$, the interactions mentioned above have lower threshold than $e^+ e^- \to \tilde{\chi}^+ \tilde{\chi}^-$ to produce $\tilde{\chi}^\pm$.

According to these considerations, a future linear collider, $e.g.$ JLC [6] will first be operated to achieve sufficiently large luminosity in the LR and RL modes which enables us to discuss in detail the physics of the Standard Model and to check small amount of discrepancy from the theory. Then, we will operate it in the LL and RR mode to search/study a special issue that would be suggested from analysis of data obtained in the LR and RL operation.

There might be long period of time and one can also expect drastic progress of accelerator technology before polarized positron beams are actually realized in future linear colliders. Therefore we attempt to create polarized e^+ on the basis of different two ideas, one of which will be later decided to adopt for future linear colliders. It is well known that e^+ emitted through β^+ decays are longitudinally polarized with the helicity v/c, v and c being the velocities of e^+ and light. Until now, one gets polarized e^+ only from β^+ decays of radioisotopes. Since numbers of e^+ from isolated radioisotopes used in off-line manner is quite limited, it is necessary to de-

velop new methods to generate large amount of polarized e^+ The first method is to use β^+ decay from radioisotopes which are produced through (p,n) interaction by means of on-line usage of a compact proton cyclotron (Fig.1) resulting in possible utilization of radioisotopes with short life-time. This method provides continuous current of e^+ , even if we use a pulse beam of protons, because the time structure of the proton beam is smeared by a decay constant of radioactive nuclei. Therefore, when we apply this method to linear colliders, we need an efficient and depolarization-free buncher. In chapter 2, details of the first method will be described.

The second method is to use $e^+ e^-$ pair creation of a polarized γ beam, which is made by backward Compton scattering of laser lights on the e^- beam supplied from a linac. We will use 1.54GeV e^- beam from the linac of the Accelerator Test Facility (ATF) that is under construction at KEK for R&D works on future linear colliders (Fig.2). The e^+ beam produced by this method has the same time structure as that of the initial laser/e^- beam. In the VLEPP project [7] and the DLC/TESLA [8] [9] project, it is also proposed [10] [11] that the polarized e^+ beams are generated by $e^+ e^-$ pair creation from polarized γ beams. The difference between the methods in these proposals and our second method is how to generate the polarized γ beam. In the VLEPP and the DLC/TESLA projects, a γ beam is generated as polarized radiation from a few hundreds GeV e^- beam which goes through a long helical undulater. Details of the second method will be described in chapter 4.

Future linear colliders require large amount of e^+ with complex time structure. For example, JLC requires intensity of 10^{14} e^+ /sec. and the pulse structure shown in Fig.3. We set a first-stage goal of development, for each method, which is reasonably realistic from technical point of view. The first step of the β^+ decay method is to create continuous e^+ beams of 10^5/sec with reasonablly good magnitude of polarizations. For the polarized γ method, we will create 10^4/sec polarized e^+ pulses with 10 Hz, whose time structure is much simpler than that of JLC. Since there are long distance between any of first stage goals and JLC requirements, many years of further efforts and innovations will be required, even if the first stage will be achieved in near future. In Chapter 5, we briefly mention the expected technical problems for realization of the polarized e^+ source of future linear colliders and some applications in the fields other than high energy $e^+ e^-$ colliders.

2 Production of polarized slow e^+'s using a compact cyclotron

2.1 Production system of slow e^+'s

The group of Sumitomo Heavy Industries, Ltd.(SHI) could successfully produce intense slow e^+ for the first time using a compact cyclotron. Recently, many laboratories have developed slow e^+ sources by means of radioisotopes (RI)[12] and an electron linear accelerator (LINAC)[13] in order to research material surfaces. Generally the former is compact and inexpensive, but the intensity of the slow e^+ is not so high, while the latter method can produce intense slow e^+ but its cost is very high and the system is normally very large.

It is expected that our slow e^+ production system using a compact cyclotron [14] will be able to provide polarized e^+ with high intensity emitted from β^+ decay radioisotopes which we produce in a nuclear reaction caused by proton irradiation of a target material. We have chosen aluminum (Al) as the target material so that the reaction $^{27}Al(p,n)^{27}Si$ with a threshold energy of 5.8 MeV takes places. The radioisotope ^{27}Si thus produced has the β^+ decay branching of 100% and a half-life of 4.1s. The large maximum energy of 3.85MeV for the β^+ rays emitted from ^{27}Si favors to achieve large helicity of e^+ because of large magnitude of v/c.

Fig. 4 shows saturated radioactivity of ^{27}Si for the proton current $1\mu A$. Using this distribution, we calculate the energy distribution of e^+ at the production point of e^+ which has enough energy to go out of Al.

The β^+ rays with wide energy spread are converted to slow e^+ with good energy resolution at a moderator. Most of the high efficiency moderators have negative-work- function, which enable us to create slow e^+ with narrow energy width (e.g.Ni(100)), or maximum yield (e.g. W, Pt). At present, we use a 25 μm thick polycrystal W foil as a moderator. However, using the Monte Carlo program SPG[15], we will make further examination to determine the most suitable thickness of W and the distance between Al and W for efficient creation of highly polarized e^+.

The calculated intensity of the slow e^+ is 4.3×10^5 slow e^+'s when a proton beam with an energy of 18 MeV and a current of $1\mu A$ irradiates an aluminum target with thickness of 1.8 mm and the slow positrons are extracted from the moderator with the conversion efficiency of 10^{-4} from β^+ rays to slow e^+. Based on this value an intensity of 3.0×10^7 slow e^+/s should be achieved using the compact cyclotron which Sumitomo Heavy Industries, Ltd. manufactures (commercial name: CYPRIS; maximum proton current: 70 μA). In addition, if the proton beam current and the conversion efficiency are improved up to 1 mA and 10^{-3} respectively in the future, it might be possible to produce a super intense e^+ beam with intensity of the order of 10^9 e^+/s. This number is the maximum of possible intensity which can be accomplished using a cyclotron and a conventional moderator.

The slow e^+ generated from the moderator are transported to the polarimeter set 27m downstream using a 100G magnetic field produced by solenoid coils. The intensity of the slow e^+ are determined by stopping all e^+ and measuring the annihilation gamma-rays with a Ge semiconductor detector. Fig. 5 shows the e^+ beam profile observed by a microchannel plate (MCP) with the diameter of 10mmϕ. The e^+ intensities of 2×10^6 e^+/s and 5×10^5 e^+/s have been obtained after the transport of 10 m and 25 m, respectively, for the proton current of 30 μA. These values are considerablly lower than the theoretical maximum intensity of 1.1×10^7 e^+/s estimated for the Al target thickness of 1.8 mm and thus the intensity should be improved in the future by refinement of various adjustments.

2.2 Helicities of slow e^+'s

In order to estimate helicities of slow e^+ emitted from the moderator, we simulate trajectories of e^+ in the Al-target and the W-moderator using the Monte Carlo program, GEANT [16]. For e^+ emitted from the Al target, we first calculate the velocity v and the angle θ at the production point, θ being the direction of e^+ measured from the z- (beam) axis. Fig. 6 (a) shows energy distributions of intial e^+ produced inside Al. Among these e^+, only high energy e^+ can pass through Al as shown in Fig. 6(b). Until now, nobody has succeeded to derive an exact formulation for the spin precession of slow e^+ in materials. However, the Michigan group clarified experimentally that no significant depolarization occurs when e^+ is moving and loosing their energies in various materials [17]. We therefore assume for the calculations of polarizations that the depolarization of e^+ does not take place during thermalization processes. If the spin directions are not changed inside the materials i.e. Al, we can determine the z component of the e^+ polarization $P_z = (v/c)cos\theta$ at

the entrance of the moderator W with the diameter 10mm placed at the distance of 10mm from the Al target. As shown in Fig. 7, we obtain an average e^+ polarization, $< P_z > = 0.68$: There exist the negative P_z which are caused by backward scattered e^+ 's. We further trace these e^+ through the moderator and check how the polarization changes. The simulation clarifies as shown in Fig. 9 that the polarization increases as the energy becomes higher. Then we will be able to extract e^+ with large polarizations if we utilize the thicker moderator which can absorb low energy e^+ (e.g. $E < 1\mathrm{MeV}$) : This was actually observed by the Michigan group [17]. We are now investigating the most suitable thickness of the W moderator by means of a Monte Carlo Simulator SPG which includes thermarization processes.

2.3 Spin precession in electric and magnetic fields

A schematic view of the experimental apparatus is shown in Fig.8. Slow e^+ 's are bunched into pulses with the time spread of 150psec, accelerated electrostatically up to 2~20KeV and injected into the polarimeter. Use of a Wien filter (spin rotator) is considered as an option to reduce possible systematic errors. The initial polarization of e^+ produced in the β^+ decay is subject to depolarization in the beam generation and transportation processes. Therefore, we have to study in detail possible depolarization at each section of the beam line. A spin precession during the beam transportation in electric and magnetic fields should be described by the relativistic theory of electromagnetism. We have developed a computer program POEM (POlarized beam simulator in Electric and Magnetic fields)[18] , based on GEANT, to simulate the trajectory and polarization of the slow positrons in static electric and magnetic fields.

The relativistic equation of motion for charged particles moving with the velocity $\vec{v}$ in the electric field $\vec{E}$ and the magnetic field $\vec{B}$ is:

$$\frac{d}{dt}(m\gamma\vec{v}) = e(\vec{E} + \vec{v} \times \frac{\vec{B}}{c}) .$$

and the spin of the particle obeys the Thomas' equation [19]

$$\frac{d\vec{s}}{dt} = \frac{e}{mc}\vec{s} \times [(\frac{g}{2} - 1 + \frac{1}{\gamma})\vec{B} - (\frac{g}{2} - 1)\frac{\gamma}{\gamma+1}(\vec{\beta} \cdot \vec{B})\vec{\beta}$$
$$-(\frac{g}{2} - \frac{\gamma}{\gamma+1})\vec{\beta} \times \vec{E}] ,$$

where $\vec{s}$ is the spin of the particle defined in the nonrotating rest system of the particle, g is the g-factor of e^+ , $\vec{\beta} = \vec{v}/c$ is the ratio of the velocity $\vec{v}$ to the speed of light c, and $\gamma = 1/\sqrt{1 - \beta^2}$. All physical quantities ($\vec{v}, \vec{B}, \vec{E}, t$) other than $\vec{s}$ are defined in the laboratory system. Eq.(2) includes contribution from the Thomas precession arising from rotation of the proper coordinate system of the particle with respect to the laboratory system. Hence the trajectory and polarization are calculated by solving the differential equations (1) and (2) using the Runge-Kutta method.

A simulation for one of the simplest cases, i.e., the beam transportation along a straight beam pipe with an axially uniform magnetic field of 100G, is performed for e^+ with the longitudinal and transverse kinetic energies of 10 eV and 1 eV, respectively. As shown in Fig.10 (a), the transverse component of the spin increases by $\sim 10^{-5}$ after the transportation of 100cm suggesting that the depolarization effect in the 27-m beam line, guided by the solenoid coils, is negligible if the beam line is straight. However, the actual beam line has seven curved sections with 90 degree of arcs of about 70cm in radii to reduce backgrounds from the cyclotron. Fig.10 (b) shows results of the simulation for the spin precession along one of the curved sections. The transverse component of the spin increases by 1.8×10^{-3} after the e^+ trajectry is bent through 90 degree of the arc. This result is consistent with the naive calculation of the effect caused by the anomalous magnetic moment of e^+ , $\frac{g-1}{2} \cdot \gamma \cdot \frac{\pi}{2}$. Therefore, we can conclude that no large depolarization occurs in our beam transportation system.

3 Measurement of the e^+ polarization

We need to design the apparatus of polarization measurement in the solenoidal beam transportating and focusing system. The mesurement of e^- polarization has been accomplished using either Mott(e^--nucleus) or Møller(e^--e^-) scattering. In principle, similar methods, i.e., Mott or Bhabha scattering could also be applied to determine the e^+ polarization. However the asymmetry, i.e., the fractional change in counting rate when a completely polarized beam has its polarization flipped, in Mott scattering of e^+ is very small, since e^+ is repelled from the nucleus. The asymmetry in Bhabha scattering are also much reduced over Møller asymmetry at energies below 1 MeV since the Pauli principle is not operative for e^+-e^- collisions.

$s_z(e^+ + e^-)$	$\lambda_{2\gamma(s_z)}$	$\lambda_{3\gamma(s_z)}$	$\lambda_{3\gamma(s_z)}/\lambda_{2\gamma(s_z=0)}$
$s_z = 1(\uparrow\Uparrow)$	forbidden	$\frac{2}{3}\cdot\bar\lambda_{3\gamma}$	$\frac{2}{3}\cdot\frac{1}{372}$
$s_z = 0(\downarrow\Uparrow)$	$\bar\lambda_{2\gamma}$	$\frac{1}{3}\cdot\bar\lambda_{3\gamma}$	$\frac{1}{3}\cdot\frac{1}{372}$

Table 1: $\uparrow$ and $\downarrow$ mean that the e^- spin is up and down, respectively. $\Uparrow$ and $\Downarrow$ the e^+ spin. $\bar\lambda_{2\gamma(s_z)}$ is the decay rate of 2γ with total spin $s_z = 0$.

We thus discuss other methods of the polarization measurement, applicable to slow e^+ under keV. In order to establish the reliable method to measure e^+ polarization, we attempt to construct measuring devices based on two different methods as described below.

3.1 Polarization measurement using a ferromagnetic target

In the case of free annihilations of unpolarized e^+ and e^- at rest, the branching ratio $B_{3\gamma/2\gamma}$ of 3γ to 2γ annihilation is represented as

$$B_{3\gamma/2\gamma} = \frac{\lambda_{3\gamma}}{\bar\lambda_{2\gamma}} = \frac{1}{372},$$

where $\bar\lambda_{2\gamma}$ and $\bar\lambda_{3\gamma}$ are the decay rates of 2γ and 3γ annihilations for unpolarized e^+ and e^-. For e^+-e^- annihilation at rest, spin states of e^+ and e^- in parallel (which is called triplet state) annihilates into 3γ, while anti-parallel spin states (which is composed of the singlet(50%) and triplet(50%) states) annihilate into 2γ and 3γ, respectively. The decay rates of the 2γ and 3γ annihilations for the total spin s_z are shown in Table 1.

The numbers of 3γ and 2γ annihilation events change by reversing the direction of e^+ spin or e^- spin. The asymmetry A is represented as

$$A = \frac{R_{para} - R_{anti-para}}{R_{para} + R_{anti-para}} \simeq \frac{4}{3}P_{e+}P_{e-} \quad (\text{for } P_{e+}P_{e-} \ll 1),$$

where R_{para} is the ratio of 3γ to 2γ annihilations of e^+ and e^- with parallel spins and $R_{anti-para}$ that with the anti-parallel spins. P_{e+} and P_{e-} stand for the polarization of e^+ and e^-, respectively.

We utilize a ferromagnetic iron-foil as a polarized e^- target. To obtain full polarization of 3d-electrons under magnetic field of 100G, the target should be very thin ($\sim 10~\mu m$). The foil is placed inclined by 20° from the beam direction to cover the full beam size (Fig.11). The parallel and anti-pallarel spin states are realized by changing the direction of the external magnetic field.

Since the ratio of numbers of polarized e^- to that of total e^- is expected to be$\sim 7\%$ in iron[20], we estimate the analysing power of the target to be 9.3%. However, it is reported that surface electrons of ferromagnetic metals are not polarized due to oxidation[21] and thus the analysing power is decreased to $\frac{1}{5}$ when 0.5 monolayer oxygen is attatched at 1×10^{-11} Torr. In order to avoid this surface effect, we should inject e^+ into inside of the target. As shown in Fig.12, 40-electrode plates are located in the vaccum chamber to accelerate e^+ up to 20 keV before e^+ is incident on the target. To suppress dispersions of the beam, Helmholz magnetic field is applied through the accelarating device.

For measurements of 4γ and 5γ decaying from a positronium, we constructed the multi-gamma ray spectrometer with 32 modules of NaI(Tl) scintillation counters[22]. On the basis of these experiences, we make a spectrometer to measure 3γ events which consists of 10 NaI(Tl) scintillation counters (diameter of 3 inch and length of 4 inch), each located on a side of a decagon with lead shields and a photomultiplier tube (Fig.13). The front face of each NaI(Tl) crystal is located at a distance of 180 mm from the center of the spectrometer. We obtain the geometrical acceptance $G \simeq 10^{-3}$ for the case that the NaI(Tl) scintillators detect simultaneously three γ-rays.

Assuming $P_{e+} = 0.5$, $G = 10^{-3}$, e^+ beam intensity $10^5 e^+/s$, and $B_{3\gamma/2\gamma} = \frac{1}{372}$, it is estimated that one week operation is necessary to determine the P within 10 % statical error.

3.2 Ortho-Positronium quenching in magnetic field

The basic idea of the polarization measurement using ortho-positronium quenching in magnetic field is described in Ref.[17],[23]. In the external

magnetic field $\vec{B}$, the singlet state of a positronium (para-Ps state) ψ_s and a sub-state of the triplet state (ortho-Ps state) $\psi_t(m = 0)$ are perturbed to form two mixed states, while other triplet sub-states, $\psi_t(m = \pm1)$ are not perturbed. Hence the mixed states are;

$$\psi'_t = \frac{1}{\sqrt{1+y^2}}\{\ \psi_t(m = 0) + y\psi_s\ \}. \qquad (3)$$

and

$$\psi'_s = \frac{1}{\sqrt{1+y^2}}\{\ \psi_s - y\psi_t(m = 0)\ \}. \qquad (4)$$

where $y = x/(1 + \sqrt{1 + x^2})$, and $x = 0.0276B$ (for B in kG) These states, ψ'_t and ψ'_s, are called an ortho-like-Ps and a para-like-Ps, respectively.

The time spectrum of Ps decays in the magnetic field B can be written as

$$\frac{dN(t)}{dt} = N_0\{\frac{1}{2}\lambda_t e^{-\lambda_t t} + \frac{1}{4}(1 - \epsilon P\cos\phi)\lambda'_t e^{-\lambda'_t t} + \frac{1}{4}(1 + \epsilon P\cos\phi)\lambda'_s e^{-\lambda'_s t}\}. \qquad (5)$$

Here, N_0 is the total number of generated Ps, $1/\lambda_t$, $1/\lambda'_t$, and $1/\lambda'_s$ are the life times of ortho-Ps ($1/\lambda_t = 140$nsec), ortho-like-Ps, and para-like-Ps, respectively and $\epsilon = x/\sqrt{1 + x^2}$. Using the field dependent parameter y, we obtain $\lambda'_t = (\lambda_t + y^2\lambda_s)/(1 + y^2)$, and $\lambda'_s = (\lambda_s + y^2\lambda_t)/(1 + y^2)$, where $1/\lambda_s = 0.125$nsec is the life time of the non-perturbed pare-Ps. The quantity P in eq.(5) is the e^+ polarization, and ϕ is the angle between the e^+ spin direction and $\vec{B}$. Number of the generated ortho-like-Ps. $N_{ortho-like}(0)$, can be determined from the shape of the time spectrum. Since $N_{ortho-like}(0)$ is related to the polarization P;

$$\frac{N_{ortho-like}(0)}{N_0} = \frac{1}{4}(1 - \epsilon P\cos\phi) \qquad (6)$$

the e^+ polarization P can be evaluated by measuring $N_{ortho-like}(0)$ for the known strength of the magnetic field. The quantity ϵ in eq.(6) is considered to be the analysing power of this method and is presented in Fig.14 as a function of B. Consequently we obtain the life time of ortho-like-Ps as a function of B as seen in Fig.15.

A schematic view of the slow e^+ polarimeter is shown in Fig.16. An e^+ beam with an energy of about 2keV enters along the magnetic field B through a hole in one of the pole pieces of the magnet and strikes the surface of a microchannel plate (MCP) target. The MCP output signal is used as the start pulse for the time measurement. A portion of the incident e^+ captures e^- 's at the surface of the MCP and then forms Ps, which, leaving the surface, annihilates into γ rays. Four modules of NaI(Tl) scintillation counters surrounding the MCP target supply stop signals when they detect γ rays.

Particular features of the magnet design is as follows;

- Magnitude of the magnetic flux density can be changed in the range between 2kG and 8kG, which is necessary to reduce systematic errors in the polarization measurement.

- Gradient of the magnetic field at the entrance to the MCP target is minimized to supress the depolarization of incident e^+ 's.

- Inhomogeneity of the magnetic field at the neighbour of the MCP target is less than 1%.

The reason why this magnet has holes in both sides of the pole pieces is to achieve better uniformity of the magnetic field and to facilitate to install the MCP. The tapered shapes of the pole pieces are to minimize the gradient of the magnetic field. The behavior of the magnetic field calculated by POISCR [24] is shown in Fig.17, where the origin of the coordinates is the center of the magnet, the z-axis is the direction of the beam line, and the r-axis points radially outword from the center of the beam lines. Fig.18 shows the systematic error expected in the polarization measurement, caused by the inhomogeneity of the magnetic field at the neighbour of the MCP target. The e^+ trajectry and the spin direction in the polarimeter are simulated, as shown in Fig.19, by POEM for the magnetic field calculated by POISCR. The simulation reveals that e^+ can reach the target with reasonablly low depolarization as seen in Fig. 19 resulting in the possible determination of the polarization with small systematic errors.

4 Polarized e^+ beam using Compton scattering

4.1 Conceptual design of the polarized e^+ beam line

As the second method to produce a highly polarized e^+ beam, we propose a relatively compact facility. Fig. 2 demonstrates the basic idea to employ Compton scattering of an unpolarized e^- beam and circularly polarized laser lights as a γ source for pair-creation. We are now preparing to produce polarized e^+ beam at the Accelerator Test Facility (ATF) for linear colliders in KEK.

The pulse-laser is required to keep enough yield of γ rays. We will use Nd:YAG laser, Continuum , NY81C-10. Its power is 550 mJ in one pulse at a wave length of 532 nm for 2 times harmonic doubler wave, and the maximum repetition rate is 10Hz. The laser light is used as 1mm diameter beam. The e^- beam of about 2×10^{10} per bunch used for our experiment is supplied from the 1.54 GeV electron linac at ATF (see Fig. 20. Though the maximum repetition rate of ATF electron linac is 25 Hz, we are going to drive it with 10 Hz as a result of limitation for the laser repetition rate. Fig. 21 shows the differential cross section for Compton scattering of unpolarized e^- with an energy of 1.54 GeV and circularly polarized lasers with 532 nm wave length. The energy distribution for the initial laser light with the helicity of -1 and the scattered γ-ray with the helicity of ± 1 are respectively shown in the figure with the dashed- and dotted-lines. The polarization of the scattered γ ray is shown as a function of the γ energies in Fig.22, where we can see that γ-rays produced at the high-end of the energy spectrum are highly polarized.

These polarized γ-rays are utilized to create polarized e^+ through pair creation on a thin target. To simplify the problem, we consider a case of incident γ-rays with a fixed energy and a fixed helicity. The differential cross section for the γ beam with an energy of 40 MeV and a helicity of $+1$ is shown as a function of the energy of produced e^- in Fig.23. The energy distribution of e^+ produced with the helicity of $+1/2$ and $-1/2$ are respectively shown by the dashed- and dotted-lines in the figure. Since the cross section is proportional to a square of a charge number Z^2 of a nucleus, we present the cross section normalized by Z^2 in the figure. The calculation is performed numerically based on the helicity amplitude in the laboratory

flame with Born approximation using HELAS[25] and BASES/SPRING[26], in which the recoiling of the nucleus and the shielding effect of e^- are not taken into account. The pair created e^+ has high polarization around the high-end of the energy distribution as shown in Fig.24.

When we required for calculation of energy and helicity distributions of e^+ created in our experiment, we have to consider that the scattered γ-ray do not have monochromatic energies. We therefore have to average over the energy and the polarization distributions of the incident (Compton scattered) γ beam. Fig. 25 shows the energy distribution of pair created e^+ weighted by the energy distributions of incident γ-rays for each helicity state with the helicity of $= \pm 1/2$. The polarization obtained in the similar manner is shown in Fig.26.

4.2 The optimization of target thickness

If we choose a thicker foil target for pair-creation, the production rate for e^+ per incident photon becomes greater, but it is necessary to consider e^+ decays and depolarizations through spin flip as a result of bremsstrahlungs in the target. For this reason, we have to determine the target thickness for pair creation to optimize the polarization and the intensity of e^+ . The calculation is performed based on the probability of various collisions and stopping forces using EGS4 and that of the spin flip using HELAS. In this simulation the e^+ converter is assumed to be Tungsten because of the large atomic number Z=74. The production rate of e^+ with various polarization values per incident photon is shown in Fig.27 indicating that the production rate of 80% polarized e^+ is saturated at 3mm, which should therefore be the best target thickness. When we want to produce higher polarization, it is necessary to take out the e^+ 's with higher energy. The lower limitation of the energy for 80% polarized positron is 43MeV as shown in Fig.27.

In the experiment designed for ATF, we will produce about 1.4×10^4 e^+ per bunch, when we take into account the power and the spot size of the laser, number of e^- per bunch , beam profile and optics of e^- .

5 Discussion and applications

We have been developing high-quality polarized e^+ beams on the basis of two new ideas which might promise us lots of interesting applications to wide areas of physics. Concerning the method of β^+ decay, it has been discussed that the beam transport system using the magnetic field might give rise to depolarization because of spiral motion of e^+. We therefore examined precisely possible process of the spin precessions in elecrtric and magnetic fields by using the simulation program POEM which we have developed according to the relativistic formalism of motion and spin precession of charged particles. In particular, we checked carefully magnitudes of depolarization in various parts of our apparatus where the magnetic field changes and consequently attributes to the spin precession. Indeed we found by POEM to be able to keep the depolarization below few percent level by adjusting the shape of magnetic fields and by accelerating e^+ to increase the ratio of the longitudinal energy to the transverse energy.

The second idea on the basis of the laser-Compton scattering leads us to realize relatively simple processes to create polarized e^+ as compared with the other methods in which the polarized γ beam are generated from a few hendred GeV e^- going through a long helical undulator. Our present attempt is certainly the first step to forecast further developments along the lines of our new idea.

One of our technical interests is to achieve polarized e^+ beams for future linear colliders which will start with the center of mass enegy 300∼500 GeV. If we want to apply the present two methods to future linear colliders, we have to surmount severe difficulties in related with the beam intensity and the bunch structure. Certainly, progress of technology in near future will be much faster than what we can now imagine and hence some of present technical difficulties will be gradually solved. Here we propose one of ideas to achieve the polarized e^+ beams for a future linear collider such as JLC based on present levels of technology.

For the first method using the β^+ decay, 3.0×10^7 slow e^+/sec is expected for a moderator with the conversion efficiency of 10^{-4} as described in Sec. 2.1. By naively extending the calculation, the production of 2.3×10^{15} e^+/sec is possible before thermalization in the moderator using a thicker (6mm) target of liquid aluminum and a high current (100mA) proton accelerator with an energy of 40MeV. Such a high current of protons may be achieved by a proton linac. It is reported that a moderator with the conversion efficiency of about 20% will possibly be available using a foil of silicon (or diamond) crystal sandwiched by electrodes which supply high electric field to extract thermalized e^+ [27]. Therefore, if we can collect 50% of e^+ emitted from the Al target in 4π solid angle and create the complex pulse structure, as shown in Fig.3, with about 50% efficiency, intensity of 10^{14} e^+/sec required in JLC can be achieved.

An idea of the buncher we propose is illustrated in Fig.28. The continuous beam of polarized e^+ is transported to the buncher with the energy of 1eV. Firstly, the e^+ beam is led to a potential gap of $V(t) = -0.04 + 0.12t + 0.0036t^2$, repeated every 6.7msec corresponding to 150Hz (Fig. 29a). Here, the time dependent potential V is in volt and the time t is in msec. Then, the beam is bunched into pulses with the time spread of about $37\mu s$ after transportation of 7620m. Secondly, the pre-bunched beam is accelerated up to 6keV to reduce space charge effect and led to the second potential gap of $V(t') = -80 + 64.9t' + 0.243t'^2$, where t' is the time in μsec. The cycle of the potential $(-18.5\mu s < t' < 18.5\mu s)$ is synchronized to the e^+ pulses of $37\mu s$ time spread coming into the second potential gap, repeated with the period of 6.7msec (Fig. 29b). The beam structure of 560ns train is obtained at 7600m downstream from the second potential gap. Then the beam is accelerated up to 200KeV which is sufficiently large as compared with the energy spread of ± 1200V before the acceleration. Finally, the accelerated beam is transported to an RF cavity with the frequency of 179MHz to produce 100 bunch structure in each of the 560ns trains. The efficiency of this buncher is possibly higher than 50%, which is able to satisfy the requirement for the polarized e^+ source described above.

For the second method using the laser Compton-scattering, hundred CO_2 laser modules would be able to create the pulse structure of JLC. As shown in Fig. 3, the JLC beam consists of 150 trains per second, each of which contains 100 bunches in the time interval of 5.6 nsec. Each bunch with a good beam quality to be forcused to the incoming e^- beam within diffraction limit has 10J and 500psec effective pulse specification. Fig. 30 shows a basic idea on the system architecture that parallel lines of pulsed CO_2 laser oscillator-amplifiers are operated sequencially at 150Hz and each line is operated with 5.6nsec. time inteval. The pulse width and timing are controlled through semiconductors switched by a module of Nd:YAG lasers of 500psec.,89MHz specificatin. The proposed laser system is well within the

reach by existing technologies of high power laser architecture, although we will have to challenge and solve lots of technical problems i.e. managements of the large system, a damage threshold of the output window and optics etc. The technical details will be described in another publication[28].

For the efficient e^+ production, we need to consider the energy of the e^- beam. If we use the CO_2 laser described above, the production rate of e^+ increases as the e^- beam energy increases and saturates above 5GeV. Adopting the CO_2 laser and the 5-GeV e^- beam, we can obtain the e^+ polarization higher than 80% if we select the e^+'s with the energy greater than 25MeV. If we assume a same capture section as that of an unpolarized e^+ source for JLC (efficiency = 40%)[29] and the transfer efficiency of the beam from the pre-damping ring to the interaction points is 50%, intensity of $1.5 \times 10^8 e^-$'s per bunch is expected at the interaction point for e^- beam with $5 \times 10^{10} e^-$'s per bunch. This is about two orders of magnitude smaller than the required value for future linear colliders. To realize the polarized e^+ beam with the designed intensity, e^- beam with $O(10^{12})$ e^-'s per bunch is needed. Our approach for achieving the required intensity is, therefore, to improve or optimize each of the system component. Use of a multiple converter target is one of candidates to be considered.

In the field other than high energy physics performed with high energy $e^+ e^-$ colliders, a polarized e^+ beam of low energy will be highly useful, too. In elementary particle physics, it is interesting to produce a large amount of polarized spin-triplet Ps by a polarized e^+ beam to study CP invariance in the lepton sector [30], being complementary to studies in high energy $e^+ e$ interactions. In solid state physics, a slow e^+ beam injected on a sample will play unique role in study of spin dependence of surface magnetism by measuring the $2\gamma/3\gamma$ decay rate of Ps [31]. In biophysics, there has been one of the biggest questions in long years that amino acids (and ribose), on which terrestrial life is based, show maximal optical activity that all amino acid (ribose) of life are L-type (D-type). Before the parity violation in weak interaction was established, the only possible explanation was that a random fluctuation in chemical and biological evolutions caused the asymmetry. On the other hand, an attractive possibility of causal mechanisms is that the parity non-conservation in the week interaction necessarily leads us to expect the selection of the L-amino acid (the D-ribose) [32]. Here, polarized e^+ beam will also be powerful tool to study this possibility [33] [34].

Finally we will briefly mention our schedule of experiments to produce the polarized e^+ beam. The various components of the apparatus for the β^+ decay method are now being constructed and tested at Tokyo Metropolitan University. Before summer, the test of all components will be finished and then the devices will be carried to the cyclotron site at SHI Examination & Inspection, LTD. Since the method of using the ferromagnetic target is, as described in sec. 3.1, subject to backgrounds arising from the decay of oPs created at the surface of the target, we might better start the polarization measurement by the quenting methods in which we can also expect large statistics.

Concerning the laser-Compton scatering, the ATF linac will be planned to operate in this autumn. We are now constructing the optics system and the detectors placed at the end of the licnac and will observe the polarization of Compton scattered γ-rays from the end of this year. In the next year, we will produce polarized e^+ and successively perform to measure the polarization of e^+ by Bhabha scattering using the ferromagnetic target.

6 Acknowledgements

References

[1] T. Omori, Y. Kurihara, K. Itoga, Y. Takauchi, M. Yoshioka, N. Nakanishi, H. Aoyagi, M. Tsubata, S. Nakamura, T. Baba, M. Mizuta, *Proc. of*

High Energy Accelerator Conference, Humburg 1992, (World Scientific, Singapore, 1992), Vol-I, p.157.

[2] H. Aoyagi, H. Horinaka, Y. Kamiya, T. Kato, T. Kosugoh, S. Nakamura, T. Nakanishi, S. Okumi, T. Saka, M. Tawada, M. Tsubata, Phys. Lett. **A167** (1992), 415.

[3] T. Maruyama, E. L. Garwin, R. Prepost, G. H. Zapaiac, J. S. Smith, J. D. Walker, Phys. Rev. Lett. **66** (1991), 2351.

[4] Y. Kurihara, T. Omori, Y. Takeuchi, M. Yoshioka, T. Nakanishi, S. Okumi, M. Tawada, K. Togawa, M. Tsubata, T. Baba, M. Mizuta, R.K. Alley, H. Aoyagi, J.E. Clendenin, J.C. Frisch, G.A. Mulhollan, P.J. Sáez, D.C. Schultz, H.Tang, K.H. Witte, Jpn. J. Appl. Phys. **34** (1995), 355.

[5] K. Flöttmann, DESY 95-064.

[6] JLC-I, JLC Group, KEK-Report 92-16(1992).

[7] V.E. Balakin, *Proceedings of ECFA workshop on e⁺e⁻ linear colliders (LC92)*, MPI-PhE/93-14 ECFA 93-154 Vol. I, (1993) pp.243, edt. R. Settles.

[8] T. Weiland, *Proceedings of ECFA workshop on e⁺e⁻ linear colliders (LC92)*, MPI-PhE/93-14 ECFA 93-154 Vol. I, (1993) pp.121, edt. R. Settles.

[9] M. Tigner *Proceedings of ECFA workshop on e⁺e⁻ linear colliders (LC92)*, MPI-PhE/93-14 ECFA 93-154 Vol. I, (1993) pp.227, edt. R. Settles.

[10] V.E. Balakin, A.A. Mikhailichenko, INP 79-85 (1979)

[11] K. Flöttmann, DESY 93-161(1993).

[12] T.Aruga, S.Takamura, M.Hirose and Y.Itoh, Phys. Rev. B 46 (1992) 14411,
G.R.Brandes, K.F.Canter and A.P.Mills, Jr., Phys. Rev. Lett. 61 (1988) 492,
W.E.Frieze, D.W.Gidley and K.G.Lynn, Phys. Rev. B 31 (1985) 5628.

[13] Y.Ito, M.Hirose, S.Takamura, O.Sueoka, I.Kanazawa, K.Mashiko, A.Ichimiya, Y.Murata, S.Okada, M.Hasegawa and T.Hyodo, Nucl. Instrum. Methods A 305 (1991) 269,
T.Akahane, T.Chiba, N.Shiotani, S.Tanigawa, T.Mikado, R.Suzuki, M.Chiwaki, T.Yamazaki and T.Tomimasu, Appl. Phys. A 51 (1990) 146,
L.D.Hulett, Jr., T.A.Lewis, D.L.Donohue and S.Pendyala, in: Positron Annihilation, Eds. L.Dorikens-Vanpraet, M.Dorikens and D.Segers (World Scientific, Singapore, 1989) p.586.

[14] M.Hirose, M.Washio and K.Takahashi, Appl. Surf. Sci. 85 (1995) 111.

[15] S. Okada and H. Kaneko, Applied Surface Science **85**, 149 (1995).

[16] *GEANT, Detector Description and Simulation Tool*, CERN Program Library Long Writeup W5013.

[17] J.Van House and P.W. Zitzewitz, Phys. Rev. A **29**, 96 (1984).

[18] T. Kumita, Preprint of TMU HEP/EXP 95-3

[19] V. Bargmann, L. Michel, and V.L. Telegdi, Phys. Rev. Lett. **2**, 435 (1959),
Classical Electrodynamics, J.D. Jackson, John Wiley & Sons.

[20] P.S.Cooper *et al.*, Phys.Rev.Lett. **34** (1975) 1589.

[21] D.W.Gidley *et al.*, Phys.Rev.Lett. **49** (1982) 1779.

[22] S. Adachi *et al.*, Phys. Rev. Lett. **65**, 2634 (1990),
S. Adachi *et al.*, Phys. Rev. A **49**, 3201 (1994).

[23] G. Gerber *et al.*, Phys. Rev. D **15**, 1189(1977),
P.W. Zitzewitz *et al.*, Phys. Rev. Lett. **43**, 1281(1979).

[24] *THE CERN-POISSON PROGRAM PACKAGE (POISCR)*, CERN Program Library Long Writeup T604.

[25] M. Murayama, I. Watanabe, K. Hagiwara, KEK Report 91-11.

[26] S. Kawabata, Compt. Phys. Commun., **41** (1986) 127.

[27] S. Tanigawa et al., RADIOISOTOPES, 41 (1992) 535 (in Japanese).

[28] Proposed method to make a highly polarized e^+ beam for future linear colliders Y. Kurihara et al., to be submitted to J.J.P.S

[29] 'ATF Design and Study Report', KEK-Internal 95-4, ed. F. Hinode et al. (1995).

[30] W. Bernreuther, U. Löw, J.P. Ma, O. Nachtmann, Z. Phys. C41, (1988) 143.

[31] D.W. Gidley, A.R. Köymen, and T.W. Capehart, Phys. Rev. Lett. 49, 1779 (1982).

[32] F. Vester, T.L.V. Ulbricht, and H. Krauss, Naturwissenschaften 46, 68 (1959).

[33] R.A. Hegstorm, Nature 297, 643 (1982), and references therein.

[34] G.W. Gidley, A. Rich, J.V. House, and P.W. Zitzewitz, Nature 297, 639 (1982), and references therein.
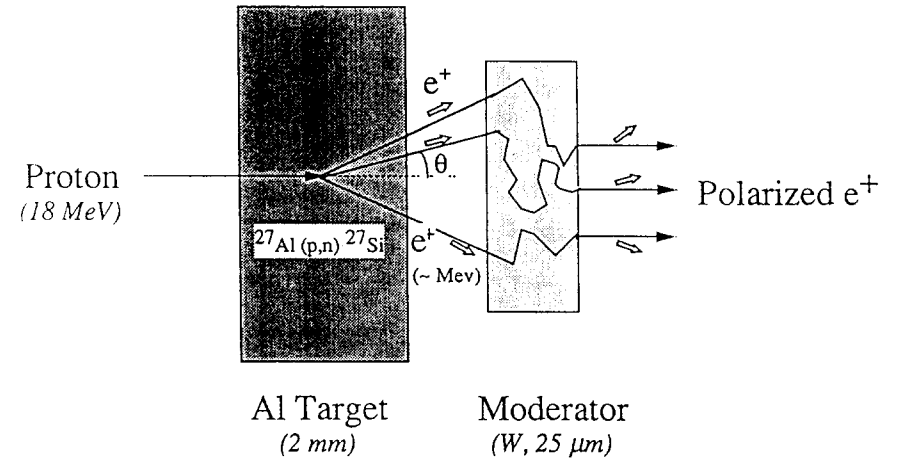
Figure 1: Polarized e^+ source using β^+ decay
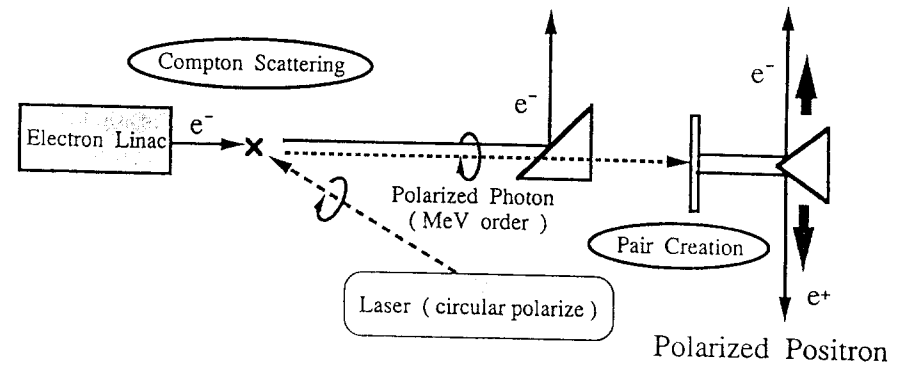
Figure 2: Polarized e^+ source using backward Compton scattering

21
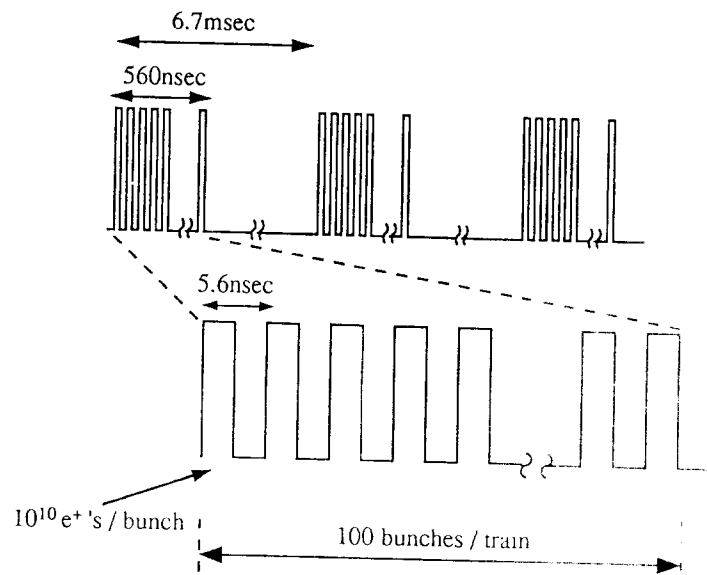
Figure 3: Time structure of the $e^{\pm}$ beams of JLC

6.7msec

560nsec

5.6nsec

$10^{10}\,e^+$'s / bunch

100 bunches / train
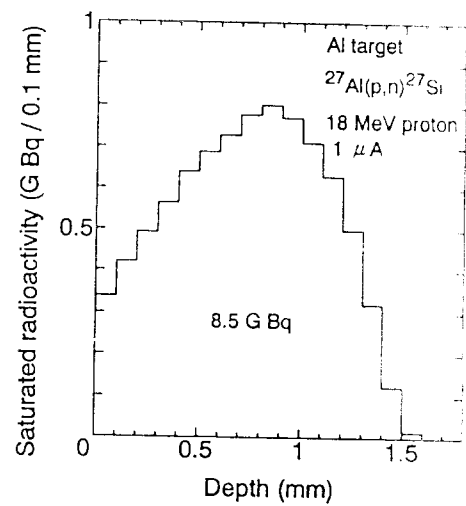
Figure 4: Saturated radioactivity of ^{27}Si

Al target
$^{27}Al(p,n)^{27}Si$
18 MeV proton
1 μA

8.5 G Bq

Saturated radioactivity (G Bq / 0.1 mm)

Depth (mm)
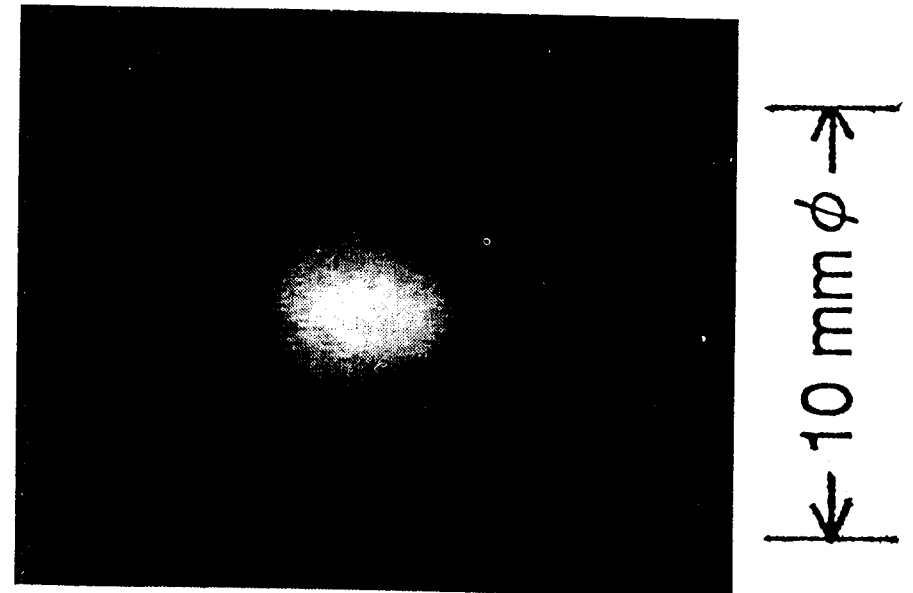
Figure 5: Positron profile

10 mm ϕ
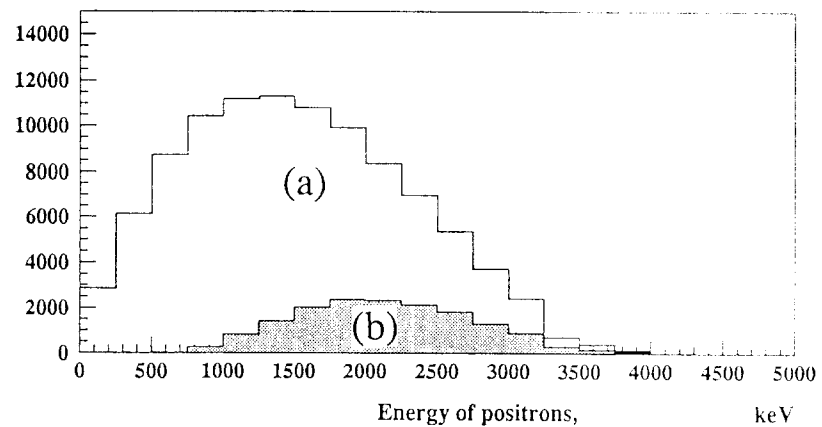
Figure 6: Energy distribution of e^+ at (a) the production points and (b) the surface of the Al target.
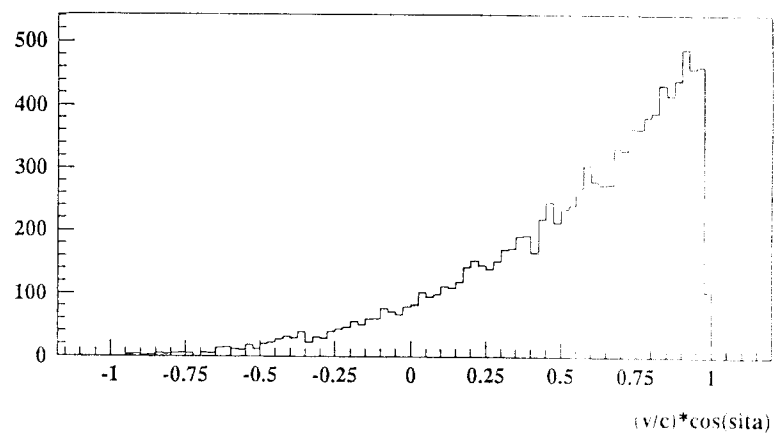
Figure 7: Polarization of e^+ along the beam direction at the entrance of the W moderator.
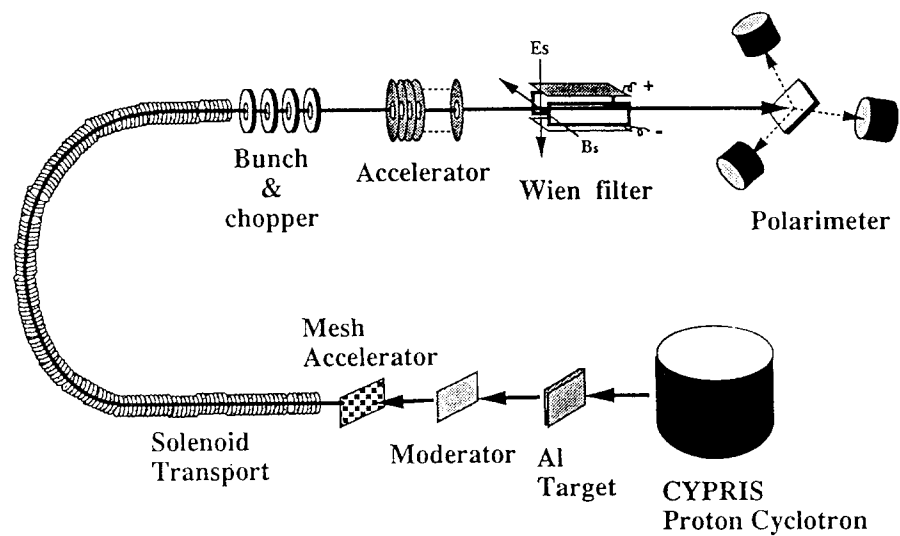
Figure 8: A schematic view of the experimental apparatus.
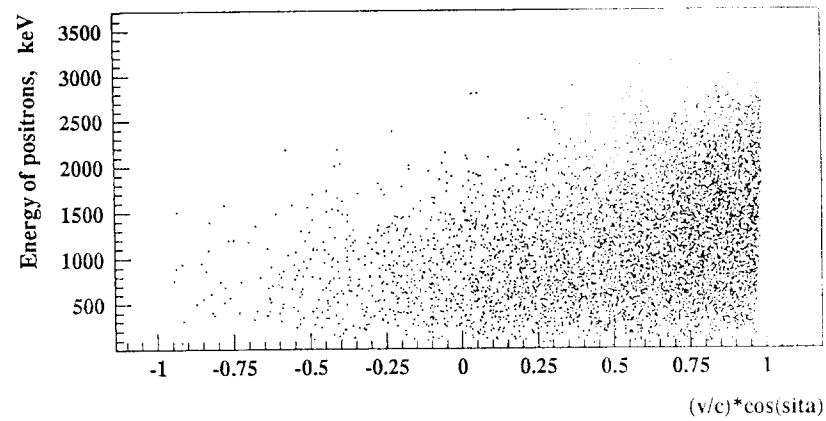
Figure 9: Correlation between energy and polarization along the beam direction.
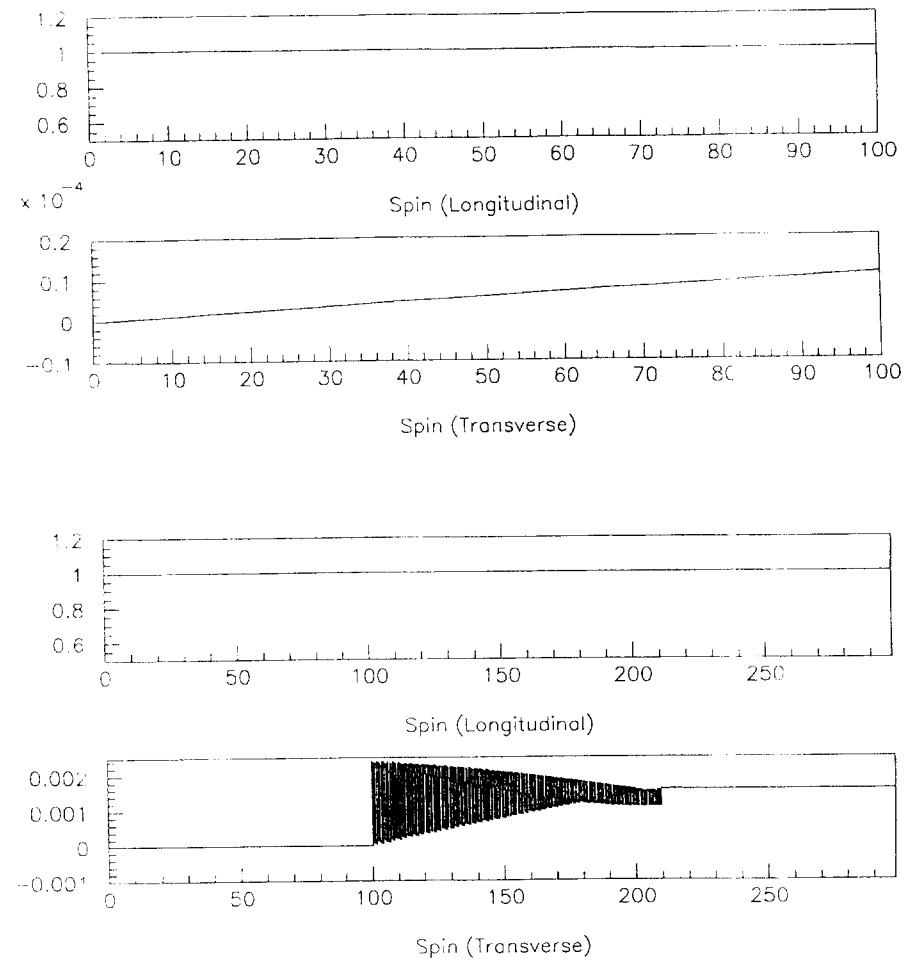
Figure 10: Spin motion calculated by POEM in the straight beam line (a) and the bent beam line (b). Longitudinal and transverse components of the spin are shown as functions of the path length in cm. Here, magnitude of the spin is normalized to unity. The curved section is between 100cm and 210cm in the path length.
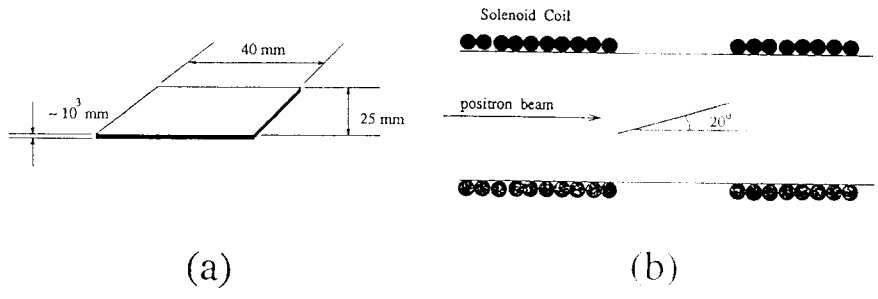
Figure 11: (a). A schematic view of the ferromagnetic iron foil target (b).The foil is inclined at 20° to the positron beam.
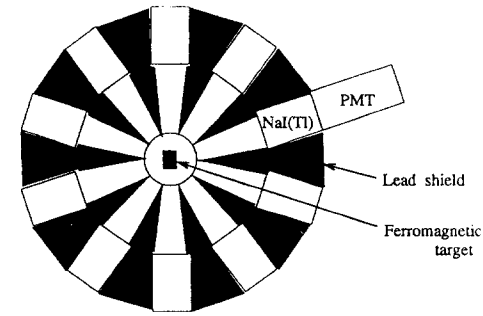
Figure 13: A cross-sectional view of the spectrometer.
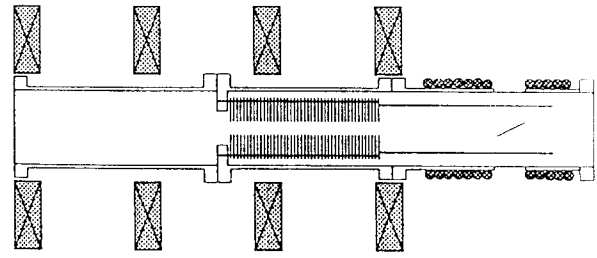
Figure 12: The vaccum chamber to accelarete the positrons up to 20 keV
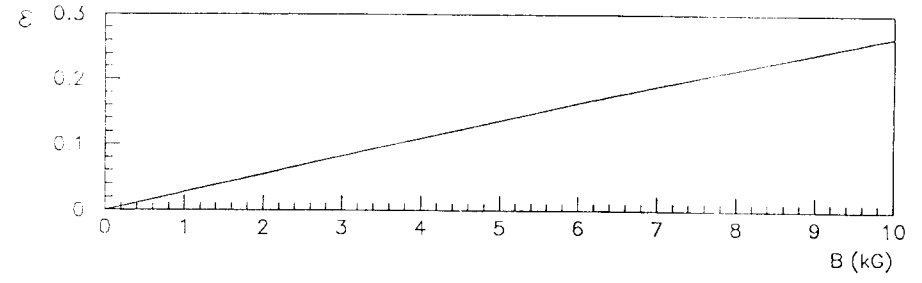
Figure 14: Analysing power ϵ as a function of the magnetic flux density B.
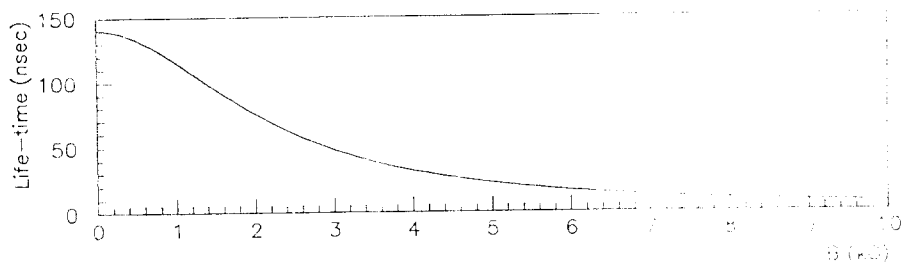
Figure 15: The relation between the magnetic flux density B and the life time of ortho-like-Ps $(1/\lambda_t)$
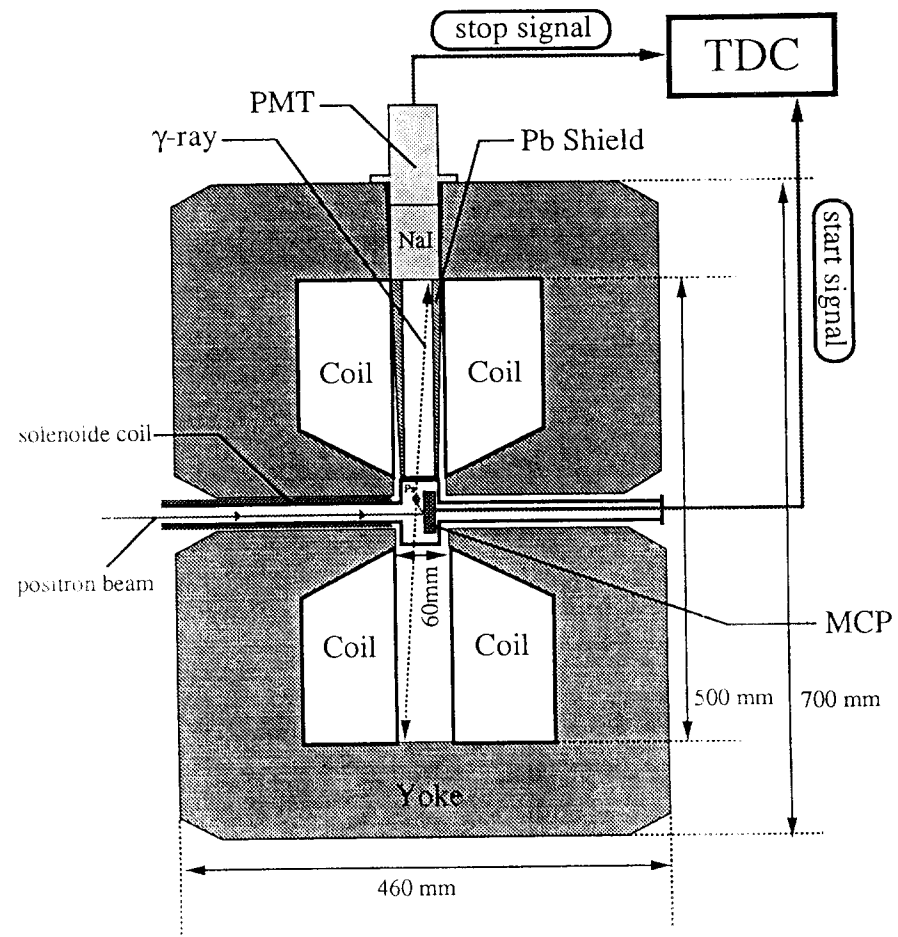
Weight : 450 kg

Figure 16: A schematic design of the polarimeter
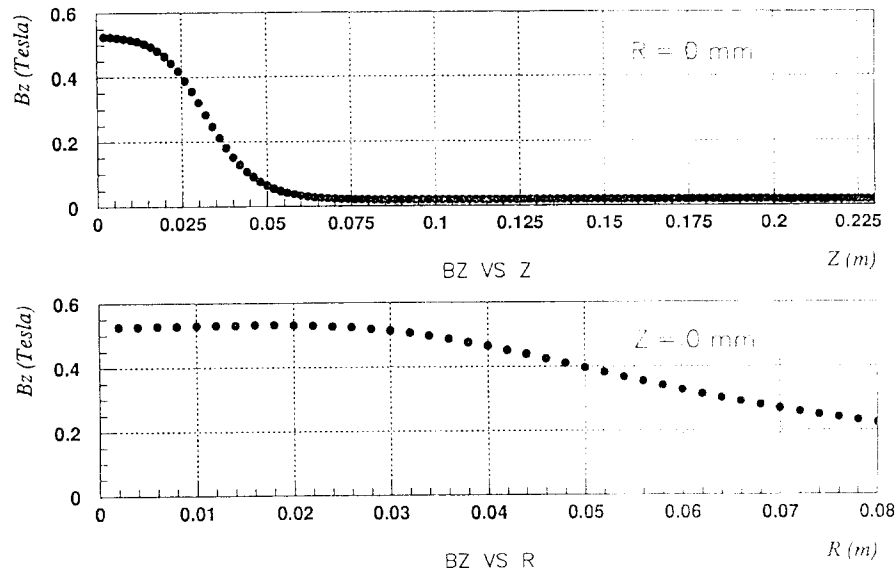
Figure 17: Magnetic flux density calculated by POISCR
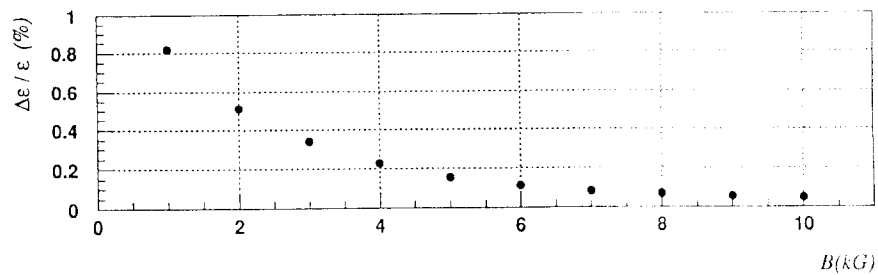
Figure 18: Expected systematic error, due to inhomogeneity of the magnetic field, as a function of the magnetic flux density B.
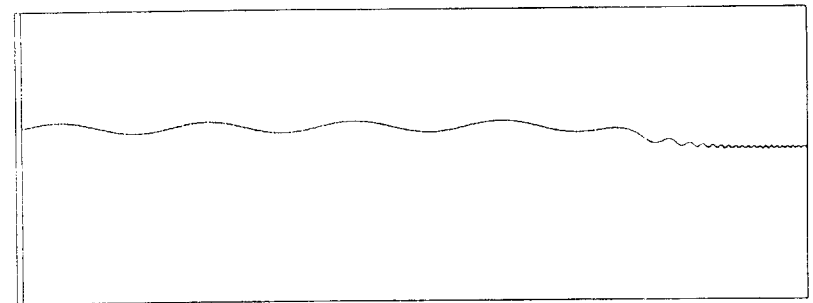
(a) Positron trajectory
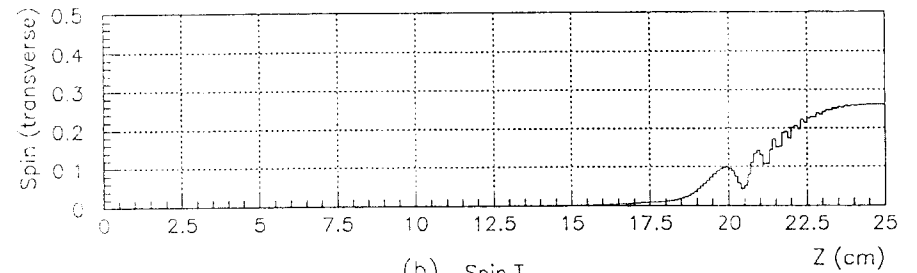
(b)   Spin T
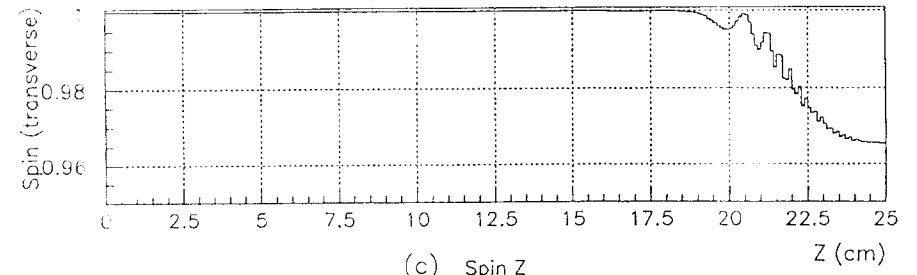
(c)   Spin Z

Figure 19: (a).Trajectory, (b).transverse componet and (c).longitudinal components of the spin simulated by POEM in the polarimeter. Here, the MCP target is placed at the right end (z=25cm). Longitudinal and transverse components of the e^+ kinetic energy are 2keV and 5eV respectively, at the entrance of the polarimeter.

ACCELERATOR TEST FACILITY FOR JLC (KEK JLC)
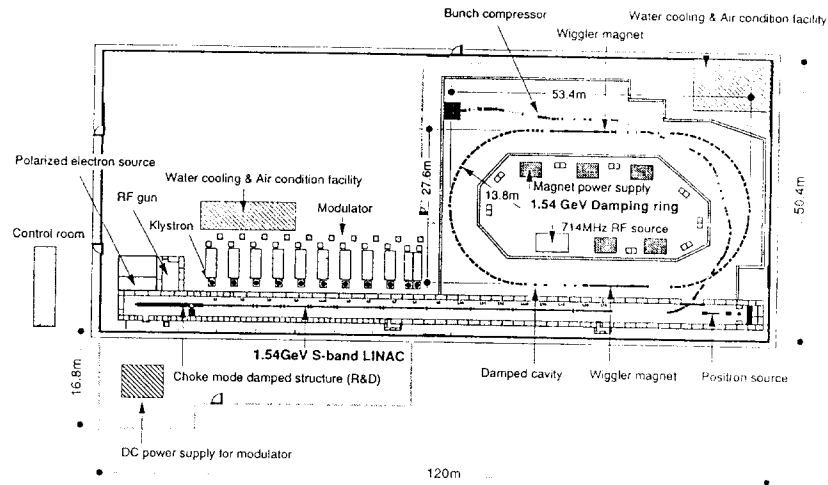
Figure 20: The Accelerator Test Facility (ATF)
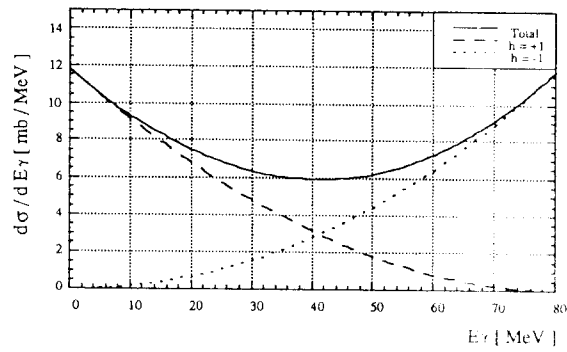
Figure 21: Differential cross section for the Compton scattering of unpolarized e^- and circularly polarized laser.
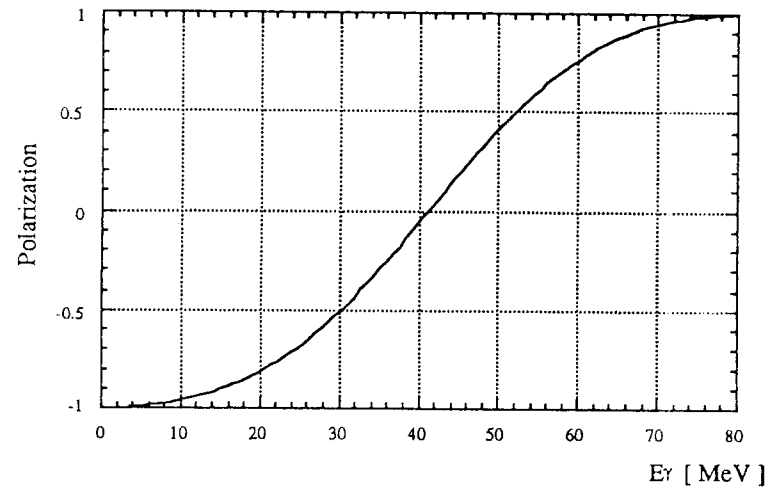
Figure 22: The polarization of the scattered γ
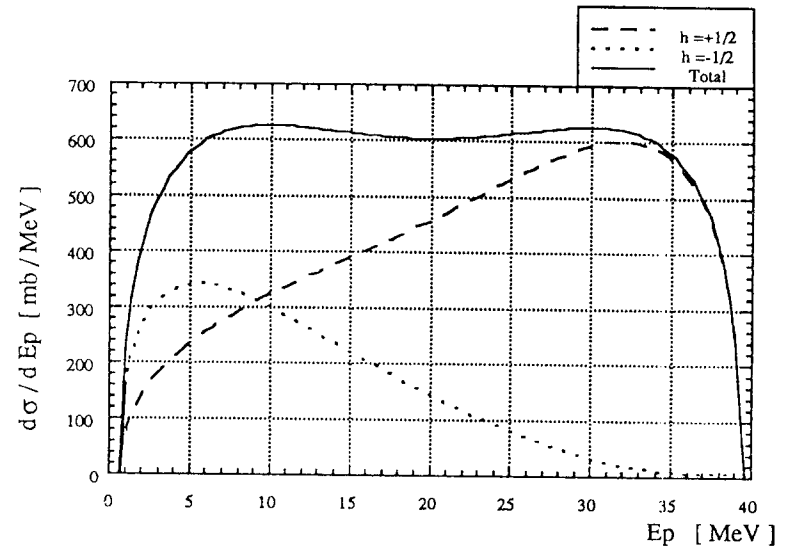
Figure 23: $d\sigma/dE$ of 40MeV photons with $h = +1$.
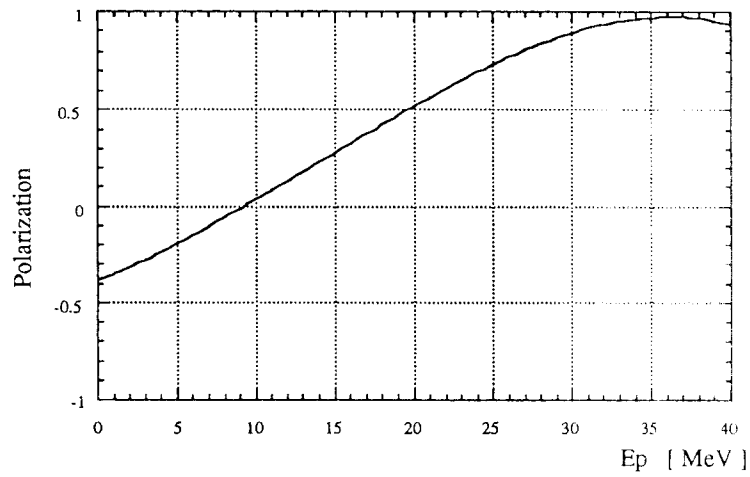
Figure 24: The polarizaation of pair-created e^+
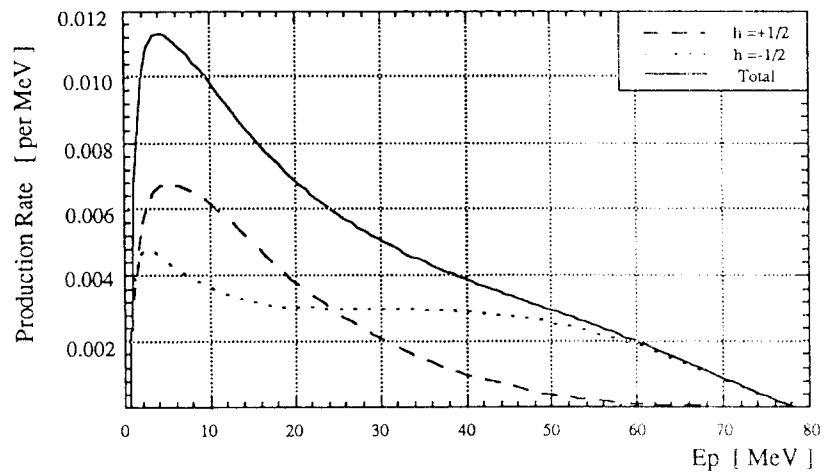

Figure 26: The resultant polarization of e^+

Figure 25: Energy distribution of e^+ $(h = \pm 1)$ weighted by the energy distribution of the incident γ.
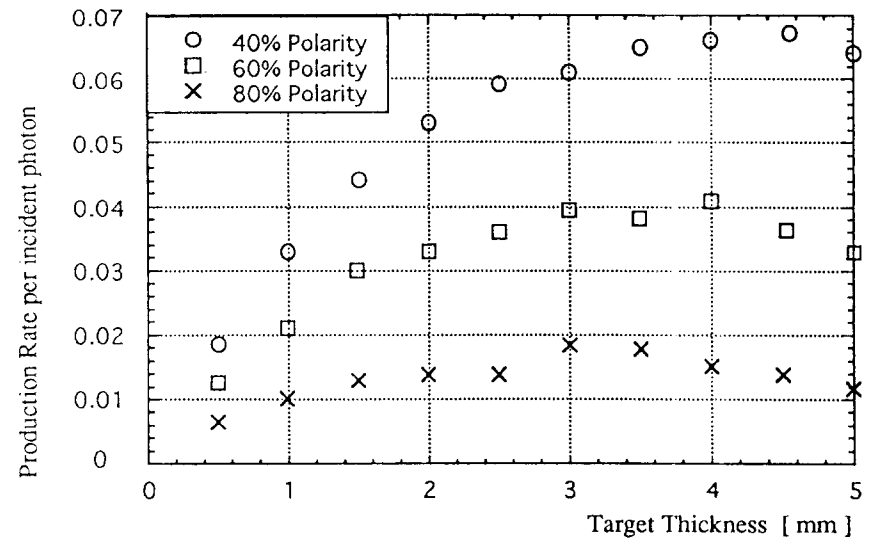

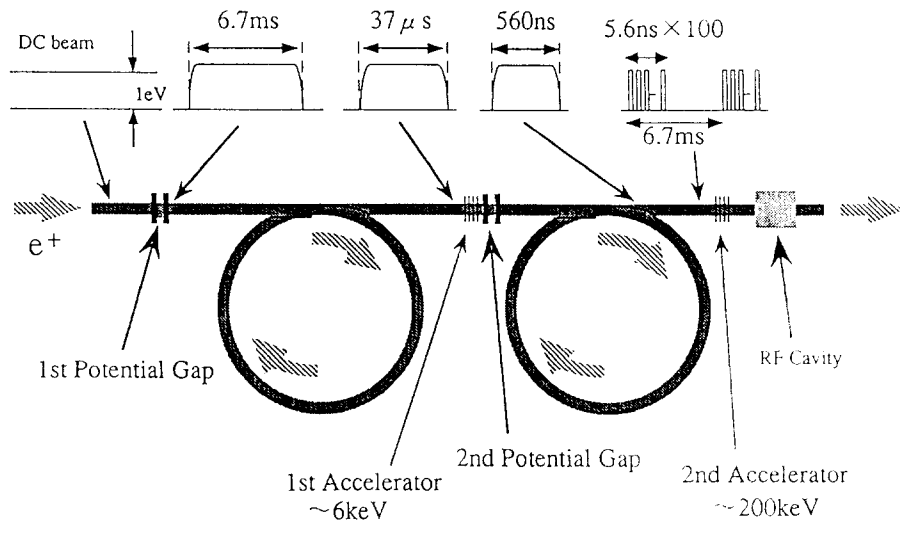Figure 27: Production rate of e^+ per photon.

Figure 28: A schematic view of the highly efficient buncher we propose. The path length along the beam line between the first potential gap and the first accelerator is 7620m, while that between the second potential gap and the second accelerator is 1300m.

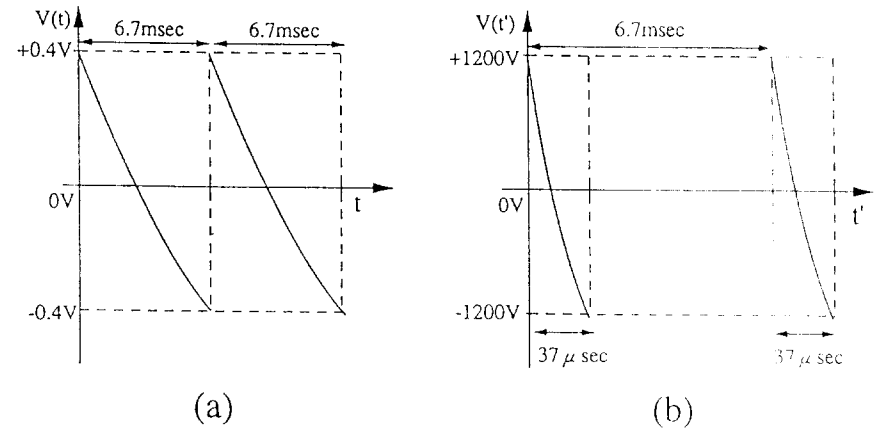(a)   (b)

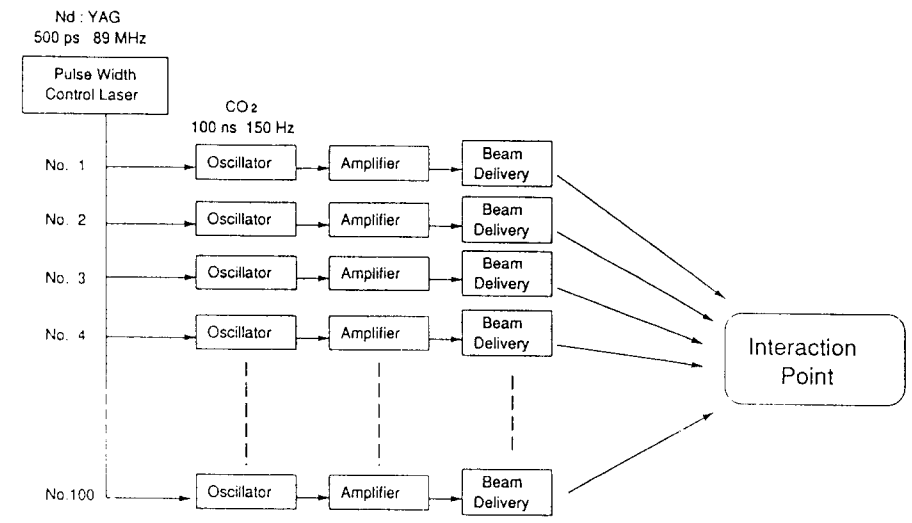Figure 29: Time dependence of (a) the first potential gap and (b) the second potential gap.

Figure 30: A schematic view of the laser system we propose.